Minimization of Reflection Error Caused by Absorbing Boundary Condition in the FDTD Simulation of Planar Transmission Lines

Krishna Naishadham, *Member, IEEE*, and Xing Ping Lin, *Member, IEEE*

***Abstract*—Residual reflection from absorbing boundaries introduces considerable error in the frequency-domain parameters of open-region planar transmission line components simulated in the time-domain. Various dispersive and super-absorbing boundary conditions have been developed to minimize this reflection. In this paper, a computationally efficient method, termed as geometry rearrangement technique (GRT), is proposed to correct the dominant reflection from absorbing boundaries by superposition of two subproblems with different source or boundary locations. The computational improvement of GRT is demonstrated by the FDTD simulation of dispersion in microstrip and coplanar transmission lines. A new method is discussed to accurately estimate the boundary reflection, and then applied to correct the characteristic impedance of planar transmission lines for boundary reflection.**

I. Introduction

SINCE THE INTRODUCTION of the finite-difference time-domain (FDTD) method by Yee in 1966 [1], it has been used by many researchers to characterize the broadband dispersive behavior of planar transmission lines and the scattering (S) parameters of passive microstrip components (cf. [2]–[5]). In order to simulate infinite space relevant to open structures, various absorbing boundary conditions (ABC) have been developed (see [6] for a comparative study of ABC applicable to waveguiding problems), with Mur's first-order ABC [7] commonly used in the FDTD analysis of planar microwave circuits. Recently, more accurate boundary conditions have been proposed, such as superabsorption [8] and perfectly matched layer (PML) [9]. Although these advancements in ABC significantly decrease the residual reflection in the time domain, they are more complicated in implementation than the simple ABC's such as Mur's. Second, the FDTD method for planar circuits is quite memory-intensive since the core memory is directly proportional to the number of cells used in the discretization of the computational volume. The computational volume can be reduced by using a low-reflection ABC such as Berenger's PML, which allows close proximity between the boundary wall and the circuit away from discontinuities.

Manuscript received October 17, 1994; revised October 2, 1995. The work was supported in part by the AFOSR Summer Research Program at Wright Laboratory, Dayton, OH, and by a Faculty Development Grant from WSU Research Council.

K. Naishadham is with the Department of Electrical Engineering, Wright State University, Dayton, OH 45435 USA.

X. P. Lin is with the TRW Transportation Electronics Division, Farmington Hills, MI 48335-2642 USA.

Publisher Item Identifier S 0018–9480(96)00465-6.

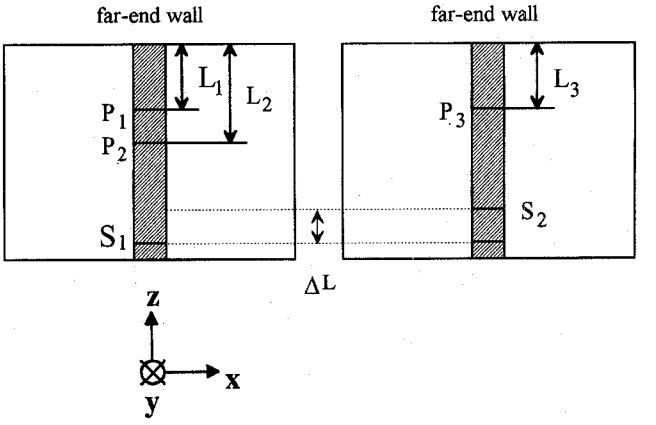

Fig. 1. Two identical transmission lines with relocation of the source in the second. The source locations S_1 and S_2 are separated by a distance ΔL.

It is possible to reduce the computational domain even for the simple Mur's ABC, *if the boundary reflection can be accurately estimated and applied to correct the computed parameters* [10], [11]. Becker [10] uses least squares minimization to estimate the dominant reflection from the far-end longitudinal boundary (Fig. 1) on a microstrip line, and invokes transmission line theory to correct the S-parameters of microstrip interconnects. Zhang *et al.* [2] employ a superposition of two subproblems with magnetic and electric walls to cancel the boundary reflection. In contrast, we employ a superposition of two subproblems, formulated by a geometrically simple rearrangement of either the exciting planar source or the absorbing boundary, to correct residual boundary reflection in the FDTD-computed parameters of planar transmission lines [11] and microstrip discontinuities [12], [13]. The procedure, termed as the geometry rearrangement technique (GRT) for convenience in further reference [11], is much simpler to implement than that in [10], because no auxiliary calculations are needed to correct the reflection error after the FDTD implementation.

In this paper, we introduce a simple procedure, based on GRT, to estimate the dominant reflection from absorbing boundary in an FDTD implementation, and describe how the reflection errors can be corrected in the effective dielectric constant (EDC) and the characteristic impedance of planar transmission lines. Although, for simplicity, we have chosen Mur's first-order ABC in the FDTD implementation, GRT can correct the error introduced by any ABC employed. The

computed results on microstrip and coplanar transmission lines indicate that the far-end longitudinal boundary can be located within 1–5 cells beyond the appropriate field sampling location, and yet, accurate results can be obtained in comparison with published data, without any necessity for curve-fitting.

The details of Yee's FDTD implementation, omitted in this paper, can be found in a few seminal articles which deal with electromagnetic field simulation of planar circuits in the time-domain [2]–[5]. In the next section, we briefly outline two different formulations of GRT, namely, source relocation and boundary relocation, to compute the effective dielectric constant. Section III describes a new technique to estimate the dominant reflection induced by the absorbing boundary. Section IV explains how the computed reflection coefficient can be employed to accurately determine the characteristic impedance. Sample results on the characterization of microstrip and coplanar transmission lines are presented in Section V, and concluding remarks are summarized in Section VI.

II. Geometry Rearrangement Technique

In the conventional FDTD method [2], the frequency-dependent EDC is calculated from Fourier-transformed voltage (or electric field) at two different points on a *single* transmission line. In order to reduce the influence of boundary reflection, the line needs to be long enough such that, ideally, only forward traveling waves exist. For convenience in notation, we will refer to this implementation as single-run FDTD (SFDTD) method to calculate the EDC. With V_1 and V_2 denoting transforms of the FDTD-computed voltage at the points P_1 and P_2 (see Fig. 1a), we have

$$e^{-\gamma(\omega)\Delta L} = \frac{V_1}{V_2} \tag{1}$$

where $\Delta L = L_2 - L_1$, $\gamma(\omega) = \alpha(\omega) + j\beta(\omega)$, $\beta(\omega) = \frac{1}{\Delta L}\angle[V_1/V_2]$. The EDC is given by

$$\epsilon_{\text{eff}}(\omega) = \frac{\beta^2(\omega)}{\omega^2\epsilon_0\mu_0} \tag{2}$$

where ω is the angular frequency and μ_0, ϵ_0 are the constitutive parameters of free space.

Equation (1) neglects the reflection error induced by an imperfect ABC. We now examine how such error influences the computed EDC. We treat the far-end wall (Fig. 1) as a lumped load at the end of the transmission line, characterized by a frequency-dependent reflection coefficient Γ_f. Likewise, the reflection coefficient at the source-end boundary is Γ_s. The remaining four walls, if absorbing, are assumed to be located far enough from the circuit (usually 2–5 strip widths away for the microstrip and about 5 slot widths away for the coplanar geometry) that their reflection can be neglected in comparison to the longitudinal reflection. The voltages V_1 and V_2 are then given by the superposition of longitudinally propagating incident wave and multiple reflections from source and far-end boundaries, and may be expressed by invoking standard transmission line theory as

$$V_1 = V_{1\text{in}}\frac{1+\Gamma_f e^{-2\tilde{\gamma}(\omega)L_1}}{1-\Gamma_f\Gamma_s e^{-2\tilde{\gamma}(\omega)L}} \tag{3}$$

$$V_2 = V_{2\text{in}}\frac{1+\Gamma_f e^{-2\tilde{\gamma}(\omega)L_2}}{1-\Gamma_f\Gamma_s e^{-2\tilde{\gamma}(\omega)L}} \tag{4}$$

where $V_{1\text{in}}$, $V_{2\text{in}}$ are incident voltages at P_1, P_2, respectively, L is the length of the line between the boundaries (Fig. 1), and $\tilde{\gamma}(\omega)$ is the true propagation constant from which EDC must be calculated. From (1), (3), and (4), we obtain

$$e^{-\gamma(\omega)\Delta L} = \frac{V_{1\text{in}}}{V_{2\text{in}}}\frac{1+\Gamma_f e^{-2\tilde{\gamma}(\omega)L_1}}{1+\Gamma_f e^{-2\tilde{\gamma}(\omega)L_2}}. \tag{5}$$

The true propagation constant should be calculated from

$$e^{-\tilde{\gamma}(\omega)\Delta L} \equiv \frac{V_{1\text{in}}}{V_{2\text{in}}} \tag{6}$$

instead of (1) or (5), which are corrupted by boundary reflection. Equation (6) follows from (5) if $L_1 = L_2$. How to realize this condition is the basis for GRT, discussed next.

A. Source Relocation GRT

The condition $L_1 = L_2$ cannot be realized on a single transmission line since the two points P_1 and P_2 coalesce into one and ΔL becomes zero. However, if two transmission lines with the same characteristics are used instead of one, as in Fig. 1, we can use voltage V_3 at point P_3 on the second line to *simulate* voltage V_2 at point P_2 on the first line. This is accomplished by relocating the *source* in the second line (identical to that in the first line) by a distance ΔL closer to the far-end boundary. Since P_3 and P_2 are equidistant from the source (Fig. 1), it follows that the incident wave amplitude $V_{3\text{in}} = V_{2\text{in}}$ and $L_3 = L_1$. The voltage V_3 is given by (4) with L_2 replaced by L_3. Expressing $V_{1\text{in}}$ and $V_{2\text{in}}$ in terms of V_1 and V_3, respectively, one obtains from (6)

$$e^{-\tilde{\gamma}(\omega)\Delta L} = \frac{V_1}{V_3}\frac{1+\Gamma_f e^{-2\tilde{\gamma}(\omega)L_3}}{1+\Gamma_f e^{-2\tilde{\gamma}(\omega)L_1}} = \frac{V_1}{V_3}. \tag{7}$$

Therefore, the result calculated from voltages sampled at P_1 and P_3, located on two identical transmission lines such that $L_3 = L_1$ (Fig. 1), is an accurate numerical result, since it does not contain the error introduced by Γ_f or Γ_s.

B. Boundary Relocation GRT

There is another way to cancel the far-end reflection, namely, to relocate the far-end boundary instead of the source on the second transmission line. This is illustrated in Fig. 2, where we observe that $V_{3\text{in}} = V_{2\text{in}}$, $L_3 = L_2 - \Delta L = L_1$, and

$$e^{-\tilde{\gamma}(\omega)\Delta L} = \frac{V_1}{V_3}\frac{1-\Gamma_f\Gamma_s e^{-2\tilde{\gamma}(\omega)L}}{1-\Gamma_f\Gamma_s e^{-2\tilde{\gamma}(\omega)(L-\Delta L)}}\frac{1+\Gamma_f e^{-2\tilde{\gamma}(\omega)L_3}}{1+\Gamma_f e^{-2\tilde{\gamma}(\omega)L_1}}. \tag{8}$$

Neglecting the composite reflection $\Gamma_f\Gamma_s$, which is small compared to unity (e.g., see Fig. 3), and using $L_3 = L_1$ (Fig. 2), it follows that

$$e^{-\tilde{\gamma}(\omega)\Delta L} = \frac{V_1}{V_3}. \tag{9}$$

Accurate propagation constant can thus be obtained with the boundary relocation technique as well. The reflection coefficient at the far-end boundary, Γ_f, can be estimated as described next.

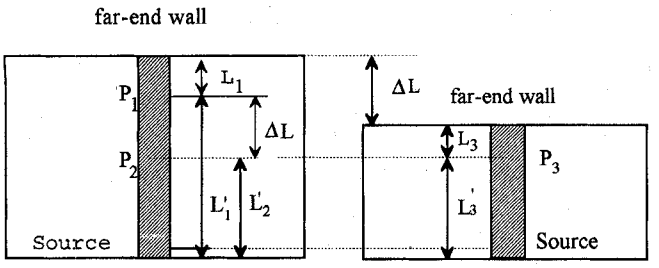

Fig. 2. Two identical transmission lines with relocation of the far-end absorbing boundary in the second. The boundary locations are separated by a distance ΔL.

III. Estimation of the Boundary Reflection

GRT can be used to estimate the boundary reflection caused by an imperfect ABC. With reference to either scheme of GRT (Fig. 1 or Fig. 2), let $C = V_1/V_2$, where V_1 and V_2 are Fourier transforms of the FDTD-computed voltage on the first line at P_1 and P_2, respectively, and $G = V_1/V_3$, with V_3 calculated on the second line at P_3. Then, we obtain from (5), (6), and (7)

$$C = G\frac{1+\Gamma_f e^{-2\tilde{\gamma}(\omega)L_1}}{1+\Gamma_f e^{-2\tilde{\gamma}(\omega)L_2}} = G\frac{1+\Gamma_f\ G^{(2L_1/\Delta L)}}{1+\Gamma_f\ G^{(2L_2/\Delta L)}}. \quad (10)$$

Solving (10) for Γ_f, we obtain

$$\Gamma_f = \frac{G-C}{G^{(2L_2/\Delta L)}C - G^{((2L_1/\Delta L)+1)}}. \quad (11)$$

The reflection coefficient at the boundary is calculated using (11). Therefore, by a simple superposition of two problems with different source or boundary locations, the frequency-dependent reflection coefficient at the boundary can be estimated.

As an example, we consider a microstrip line with dielectric constant $\epsilon_r = 2.2$, strip width $W = 2.394$ mm, and substrate thickness $h = 0.795$ mm. Two transmission lines are simulated, with one line 120 cells long and the other 90 cells long. Both are terminated with Mur's first-order ABC [7]. The longer line is simulated to obtain C and the shorter one, to calculate G. The cell dimensions are given by $\Delta x = 0.399$ mm, $\Delta y = 0.265$ mm, and $\Delta z = 0.40$ mm (see Fig. 1 for definition of coordinates). The number of cells along x and y directions, respectively, is given by $N_x = 60$ and $N_y = 15$. The other dimensions are: $L_1 = L_3 = 10\Delta z$, $\Delta L = 30\Delta z$, and $L_2 = 40\Delta z$. The magnitude of the Mur's first-order boundary reflection coefficient, calculated from (11) using the boundary relocation GRT, is shown in Fig. 3. Also shown for comparison is an independent result, obtained using the spectral domain Prony's method [14]. Prony's method computes the reflection coefficient directly without the need for solving two auxiliary problems. The GRT (or the present) and Prony's results are in good agreement, and predict that Mur's ABC causes about -32 dB of reflection for the microstrip geometry. The GRT result clearly shows the periodic oscillatory behavior of the reflection coefficient as a function of frequency.

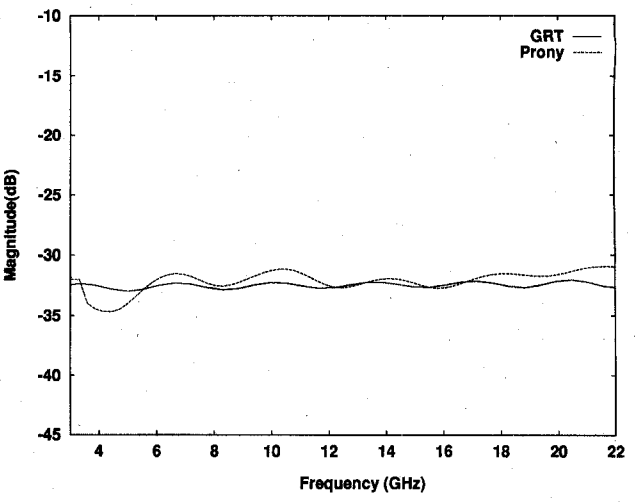

Fig. 3. Reflection coefficientfor Mur's first-order ABC applied to the microstrip geometry.

IV. Characteristic Impedance

Once the reflection coefficient at the location of the absorbing boundary is estimated, it can be used to correct the computed parameters for the reflection error. We now describe how such a correction can be accomplished for the characteristic impedance. With reference to Fig. 1, the current at the location P_1 is given by

$$I_1 = I_{1\text{in}}\frac{1-\Gamma_f e^{-2\tilde{\gamma}(\omega)L_1}}{1-\Gamma_f\Gamma_s e^{-2\tilde{\gamma}(\omega)L}} \quad (12)$$

where $I_{1\text{in}}$ is the complex incident current in the plane P_1. The net complex current I_1 is determined by integrating the frequency-domain magnetic field intensity along a rectangular contour in plane P_1 described around the transmission line conductor. Expressing $V_{1\text{in}}$ in terms of V_1 using (3), and $I_{1\text{in}}$ in terms of I_1 using (12), one obtains the charactristic impedance

$$Z_0 \equiv \frac{V_{1\text{in}}}{I_{1\text{in}}} = \frac{V_1}{I_1}\frac{1-\Gamma_f e^{-2\tilde{\gamma}(\omega)L_1}}{1+\Gamma_f e^{-2\tilde{\gamma}(\omega)L_1}}. \quad (13)$$

Because the voltage and current reflection coefficients differ in sign, it is evident that the boundary reflection cannot be canceled for Z_0 by a simple rearrangement of geometry described in Section II for the EDC. Instead, Γ_f is estimated as described in Section III, and then substituted in (13) to correct the characteristic impedance. In the conventional FDTD implementation, the characteristic impedance is computed from the net voltage V_1 and the net current I_1 as

$$Z_0 = \frac{V_1}{I_1} \quad (14)$$

which is subject to error introduced by boundary reflection.

V. Test Results

A. Effective Dielectric Constant

We have calculated the effective dielectric constant of a microstrip line using the source relocation GRT, and a coplanar waveguide (CPW) using the boundary relocation GRT. The

TABLE I
COMPUTATIONAL PARAMETERS

Parameter	Microstrip Line	CPW
Substrate dielectric constant	13.0	12.9
Thickness of the substrate (mm)	0.1	0.5
Width of the center strip (mm)	0.15	0.135
Width of the lateral strips (mm)		0.59
Slot width (mm)		0.065
Cell size $\Delta x = \Delta y = \Delta z$ (mm)	0.0125	0.0135
Time step Δt (ps)	0.0215	0.0176
Numbers of cells (GRT) $N_x \times N_y \times N_z$	$55 \times 30 \times 30$	$60 \times 55 \times 60$
Number of cells (SFDTD) $N_x \times N_y \times N_z$	$55 \times 30 \times 160$	$60 \times 55 \times 160$
Number of time steps	4096	4096

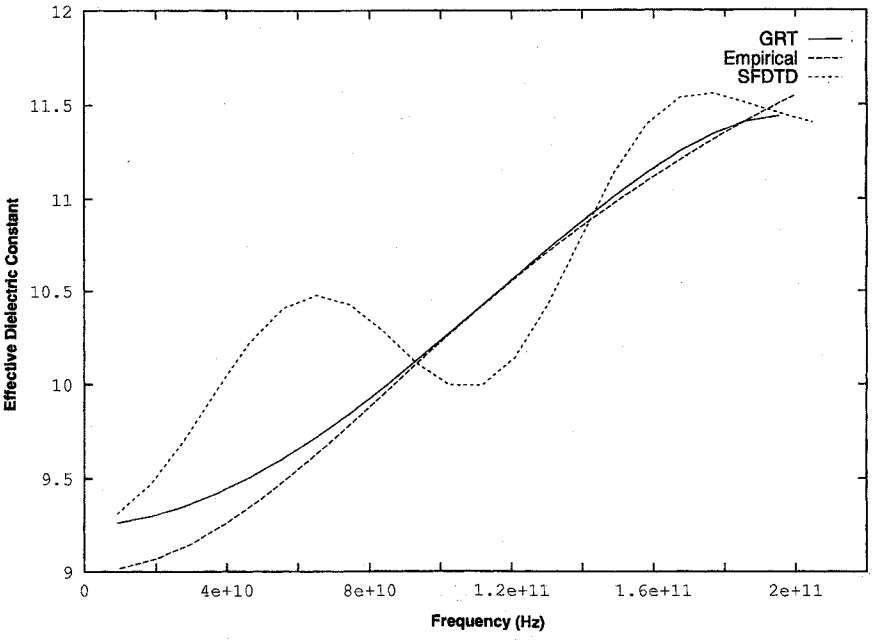

Fig. 4. Frequency-dependent effective dielectric constant of the microstrip transmission line.

parameters used in the two computations are summarized in Table I. The same microstrip line has been analyzed by Zhang *et al.* [2] using the FDTD method. They have minimized the reflection error from ABC by superposing the solution of two subproblems whose domains are terminated by electric and magnetic walls, respectively. However, they use 160 cells longitudinally for each subproblem in order to reduce the interference from the walls. In contrast, the GRT/FDTD implementation employs only 30 cells longitudinally for each of the subproblems in Fig. 1, thereby achieving at least five-fold savings in computer memory and CPU time. We employ first-order Mur's ABC on all the walls except the ground plane. A planar Gaussian pulse specified by

$$E_z = \exp -\{(t - t_0)/\ T\}^2 \tag{15}$$

where $t_0 = 150\Delta t$, $T = 50\Delta t$, excites the field 10 cells away from the $z = 0$ plane. The computed results are shown in Fig. 4. The conventional (or SFDTD result) shows periodic oscillation around the GRT result, caused by boundary reflection. The GRT result is quite smooth and agrees very well (within 1%) with the empirical formula of Edwards and Owen [15], and with the FDTD result computed in [2]. It is emphasized that no curve-fitting has been employed to generate the smooth curve for GRT.

Next, we characterize the dispersion in a CPW, whose parameters are displayed in Table I. The same geometry has been analyzed by using FDTD in [16]. However, instead of using the time-consuming superabsorption boundary condition, we employ the simple first-order Mur's ABC on all the walls, and correct the ensuing errors.

The numerical results for the CPW are shown in Fig. 5. Four curves are shown—the conventional (or SFDTD) result,

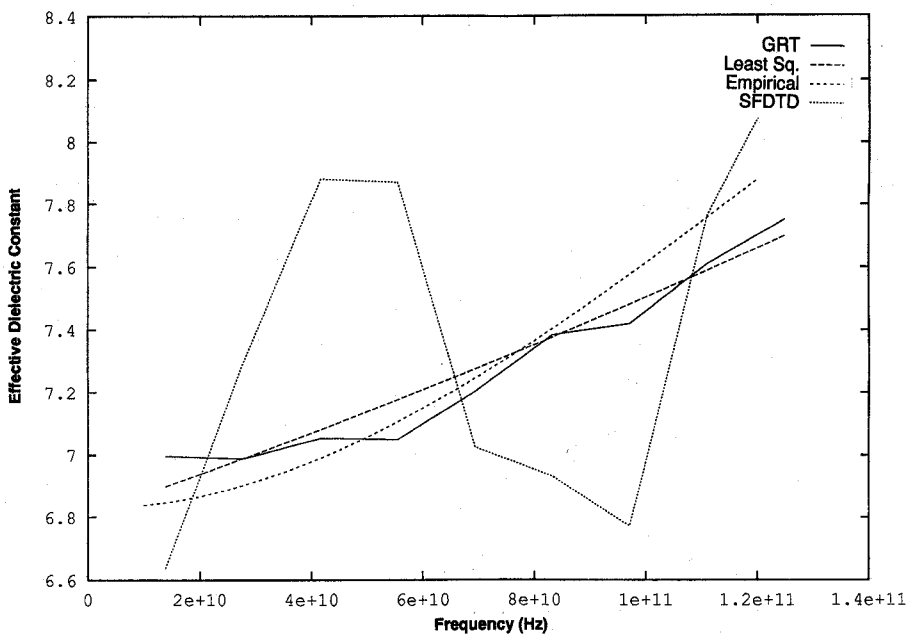

Fig. 5. Frequency-dependent effective dielectric constant of the coplanar transmission line.

the GRT result, the least squares fit to the GRT data, and Whinnery's empirical formula [17]. It is observed that the maximum deviation between the GRT data and their least squares fit is less than 1.5%. The SFDTD result, on the other hand, oscillates around these two curves, and produces more than 12% deviation from the least squares fit to the GRT data. The least squares fit agrees reasonably well with the empirical formula, the error between the two being less than 1% up to about 100 GHz. Therefore, considerable improvement in computational accuracy of the EDC can be achieved, even for the CPW, by using GRT with a simple absorbing boundary condition instead of the conventional SFDTD implementation. With regard to the superabsorbing boundary condition, the present approach is faster, but, it does not correct the error resulting from boundaries other than longitudinal. This error accounts for the small oscillation in the GRT result. However, upon comparison of the SFDTD and GRT results, it seems that reflection from the longitudinal wall is still the main contributor to the error in SFDTD method.

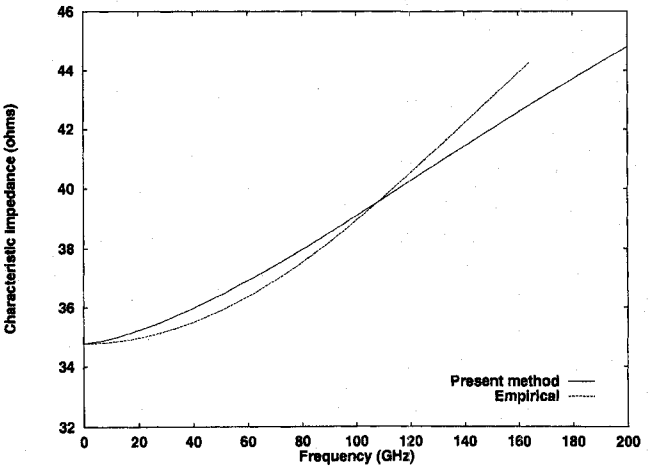

Fig. 6. Frequency-dependent characteristic impedance of the microstrip transmission line.

B. Characteristic Impedance

Fig. 6 displays the frequency-dependent characteristic impedance of a microstrip line with the same geometrical parameters as shown in Table I. The impedance has been computed using (13), and, as such, is corrected for boundary reflection. For comparison, the result of an empirical formula from [18] is also shown. The FDTD-computed impedance approaches closely the quasistatic DC limit predicted by the empirical dispersion model, and the two results are within 2% up to about 140 GHz. The empirical model is not valid beyond the cut-off frequency of the first transverse electric (TE) mode, which occurs at 155 GHz. Within its range of validity, the empirical model is believed to be about 2% accurate [19]. Our FDTD-computed characteristic impedance is found to be in good agreement with the corresponding curve in Fig. 6 of [2] over the entire frequency range of 200 GHz.

The characteristic impedance for the CPW listed in Table I is computed by the FDTD method and compared in Fig. 7 with the correponding result from Fig. 6(a) of [16]. Good agreement between the two results is gratifying, given that the computational domain of the present method is about a fifth smaller than the domain in [16], and reinforces confidence in the capability of the present method to compensate for boundary reflection error.

VI. Conclusion

We have presented a simple method for the correction of ABC-induced error in the FDTD analysis of planar transmission line components. GRT involves the solution of two sub-

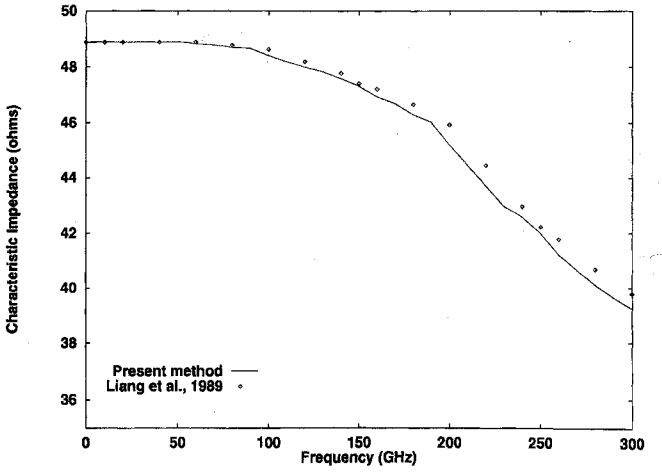

Fig. 7. Frequency-dependent characteristic impedance of the coplanar transmission line.

problems differing in geometry only in the position of either the far-end longitudinal boundary or the exciting source. The computational requirements of GRT are less than those of the conventional FDTD implementation, in which the absorbing boundary needs to be placed far away from the circuit element to reduce the boundary-circuit interaction. We have introduced a new method to estimate the boundary reflection coefficient and correct the computed circuit parameters. GRT with a simple first-order ABC has been employed to characterize the dispersion in EDC and characteristic impedance of planar transmission lines, and good agreement has been established between the computed and published results.

It is emphasized that the computational savings are most significant when GRT is applied to discontinuity problems. We have used GRT to compute the S-parameters of a microstrip filter [11], a microstrip bend [13], CPW discontinuities and filter elements [20]. In all cases, we have observed good corroboration between computed and measured results.

REFERENCES

[1] K. S. Yee, "Numerical solution of initial boundary value problems involving Maxwell's equations in isotropic media," *IEEE Trans. Antennas Propagat.*, vol. AP-14, pp. 302–307, May 1966.

[2] X. Zhang, J. Fang, and K. K. Mei, "Calculations of the dispersive characteristics of microstrips by the time-domain finite-difference method," *IEEE Trans. Microwave Theory Tech.*, vol. MTT-36, pp. 263–267, Feb. 1988.

[3] T. Shibata, T. Hayashi, and T. Kimura, "Analysis of microstrip circuits using three-dimensional full-wave electromagnetic field analysis in the time domain," *IEEE Trans. Microwave Theory Tech.*, vol. MTT-36, pp. 1064–1070, June 1988.

[4] X. Zhang and K. K. Mei, "Time-domain finite difference approach to the calculation of the frequency-dependent characteristics of microstrip discontinuities," *IEEE Trans. Microwave Theory Tech.*, vol. MTT-36, pp. 1775–1787, Dec. 1988.

[5] D. M. Sheen, S. M. Ali, M. D. Abouzahra, and J. A. Kong, "Application of the three-dimensional finite-difference time-domain method to the analysis of planar microstrip circuits," *IEEE Trans. Microwave Theory Tech.*, vol. MTT-38, pp. 849–857, July 1990.

[6] V. Betz and R. Mittra, "Comparison and evaluation of boundary conditions for the absorption of guided waves in an FDTD simulation," *IEEE Microwave Guided Wave Let.*, vol. 2, pp. 499–501, Dec. 1992.

[7] G. Mur, "Absorbing boundary conditions for the finite difference approximation of the time domain electromagnetic field equations," *IEEE Trans. Electromagn. Compat.*, vol. EMC-23, pp. 377–382. Nov. 1981.

[8] K. K. Mei and J. Fang, "Superabsorption—A method to improve absorbing boundary conditions," *IEEE Trans. Antennas Propagat.*, vol. AP-40, pp. 1001–1010, Sept. 1992.

[9] J. Berenger, "A perfectly matched layer for the absorption of electromagnetic waves," *J. Comp. Phys.*, vol. 114, no. 2, pp. 185–200, Oct. 1994.

[10] W. D. Becker, "The application of time-domain electromagnetic field solvers to computer package analysis and design," Ph.D. dissertation, Dept. Elec. Eng., Univ. of Illinois at Urbana-Champaign, 1993.

[11] K. Naishadham and X. P. Lin, "Geometry rearrangement technique—A new method to minimize reflection from absorbing boundaries in the FDTD analysis of planar transmission components," in *Proc. 24th European Microwave Conf.*, Cannes, France, Sept. 1994, vol. 2, pp. 1547–1552.

[12] X. P. Lin and K. Naishadham, "A simple technique for minimization of ABC-induced error in the FDTD analysis of microstrip discontinuities," *IEEE Microwave Guided Wave Let.*, vol. 4, pp. 402–404, Dec. 1994.

[13] K. Naishadham and X. P. Lin, "A study of the optimum compensation of open microstrip discontinuities using the FDTD method with boundary reflection error cancellation," *Int. J. Microwave and Millimeter-Wave CAE*, vol. 6, 1996 (in press).

[14] ——, "Application of spectral domain Prony's method to the FDTD analysis of planar microstrip circuits," *IEEE Trans. Microwave Theory Tech.*, vol. MTT-42, pp. 2391–2398, Dec. 1994.

[15] T. C. Edwards and R. P. Owen, "2–18 GHz dispersion measurements on 10–100 ohm microstrip line on sapphire," *IEEE Trans. Microwave Theory Tech.*, vol. MTT-24, pp. 506–513, 1976.

[16] G. Liang, Y. Liu, and K. K. Mei, "Full-wave analysis of coplanar waveguide and slotline using the time-domain finite-difference method," *IEEE Trans. Microwave Theory Tech.*, vol. 37, pp. 1949–1957, Dec. 1989.

[17] G. Hasnain, A. Dienes, and J. R. Whinnery, "Dispersion of picosecond pulses in coplanar transmission lines," *IEEE Trans. Microwave Theory Tech.*, vol. MTT-34, pp. 738–741, June 1986.

[18] P. Pramanick and P. Bhartia, "An accurate description of dispersion in microstrip," *Microwave J.*, pp. 89–96, Dec. 1983.

[19] R. A. York and R. C. Compton, "Experimental evaluation of existing CAD models for microstrip dispersion," *IEEE Trans. Microwave Theory Tech.*, vol. 38, pp. 327–328, Mar. 1990.

[20] X. P. Lin, "Efficient analysis of passive microwave circuits using the finite-difference time-domain method," M.S. thesis, Dept. Elec. Eng., Wright State Univ., Aug. 1994.

Krishna Naishadham (S'83-M'87) received the M.S. degree from Syracuse University, and the Ph.D. degree from the University of Mississippi, both in electrical engineering, in 1982 and 1987, respectively.

From 1987 to 1990, he was an Assistant Professor in Electrical Engineering at the University of Kentucky, Lexington. In 1990 he joined the Department of Electrical Engineering at Wright State University, where he is currently an Associate Professor. His research interests are in the areas of computational electromagnetics, design and analysis of microwave and millimeter-wave integrated circuits (MMIC's), prediction of EMI in printed circuit boards and electronic packages, and electronic materials. He is an AFOSR-sponsored Visiting Scientist at Wright Laboratory, Dayton, since 1992, where he has worked on EM simulation of MMIC's, and on microwave characterization of high-temperature superconducting thin films. He has published over 60 papers in professional journals and conference proceedings on these topics.

Dr. Naishadham is a member of Eta Kappa Nu and Phi Kappa Phi, and an elected member of URSI Commission B. He serves on the Digital Signal Processing and Numerical Methods Committees of IEEE Microwave Theory and Techniques Society. He received the Best Session Paper award at the 7th SAMPE Conference on Electronic Materials.

Xing Ping Lin (S'94-M'95) received the M.S. degree in electrical engineering at Wright State University in 1994, where he was a Research Assistant from 1993 to 1994. His thesis dealt with efficiency issues for the simulation of MMIC's using the finite-difference time-domain method.

Since November 1994, he has been an RF Design Engineer at the TRW Transportation Electronics Division.